ANALYSIS OF THE HORIZONTAL EFFECTIVE THERMAL CONDUCTIVITY OF A FLUIDIZED ALUMINA BED UNDER STEADY-STATE CONDITIONS

L. E. Krigman and A. P. Baskakov

UDC 536.2:541.182

A critical relation is derived for calculating the thermal conductivity of a fluidized alumina bed. Based on the solution to the equation, formulas are then derived for evaluating the nonuniformity factor of the temperature field in a fluidization chamber which is heated around its walls.

When heat is supplied from the sidewalls of a fluidizing chamber which are spaced far from the center, a nonuniform transverse temperature field will be established in that chamber. The degree of nonuniformity, an evaluation of which is necessary for the design of industrial apparatus, depends on the chamber dimensions as well as on the effective thermal conductivity of the fluidized bed. The data published so far on the horizontal effective thermal conductivity of fluidized beds are of no use in evaluating the nonuniformity of the temperature field in a large chamber, since studies, although most thorough, have been made on scaled-down models. At the same time, it is well known that the heat-transfer coefficients increase drastically as the chamber dimensions become larger (see [1, 2]). For this reason, considering that practical problems must be solved which arise in the design of a large furnace with a boiling bed, the authors have studied the horizontal effective thermal conductivity of a scaled-up fluidized alumina bed.

The study was conducted under steady-state conditions. This made it possible to avoid a number of shortcomings [2] inherent in the heat-pulse method [3, 4, 5].

For the experiment we used a slitted chamber 1000 × 70 mm and 1500 mm high, lined with fireclay brick 230 mm thick (113 mm at the top). Ambient air was supplied from underneath through a 1% active area in the solidly sintered grate (Fig. 1). The heat source was a 2.4 kW electric heater immersed in the bed near the endwall. Six Chromel–Alumel control thermocouples and six Chromel–Copel measuring thermocouples were installed in the chamber with their hot junctions 80 mm above the grate.

The horizontal distance between the measuring thermocouples was 130 mm. Their cold junctions were connected through a switch to a KP-59 potentiometer. The air rate was checked by means of a flowmeter diaphragm and a cup-shaped model MMN micromanometer. The material used in the test was deaerated alumina having a density of 3.65 g/cm^3 and the grain-size distribution (determined by a microscopic analysis with an MIM-7 instrument) shown in Table 1.

The porosity of the solid (unrammed) bed was $\varepsilon_0 \approx 0.7$.

The use of a slitted chamber in the experiments made it possible, according to Lehman's analysis in [6], to obtain the values of the heat-transfer coefficients close to their maximum for a given bed height, as long as the bed height was smaller than the length of the chamber and the slit was not wider than 100 mm. In this way, the nonuniformity of the temperature field in an industrial furnace could be evaluated quantitatively from the test results obtained with a long, slitted chamber.

The tests were performed with interstitial velocities ranging from 0.14 to 0.38 m/sec. The velocity at which fluidization began was determined experimentally and found to be 0.06 m/sec at an air temperature of 11°C. The mean temperature of the bed varied between 40 and 190°C depending on the air velocity

Yuzh NIIGIPROGaz, Donetsk. Translated from Inzhenerno-Fizicheskii Zhurnal, Vol. 21, No. 2, pp. 301-308, August, 1971. Original article submitted October 9, 1970.

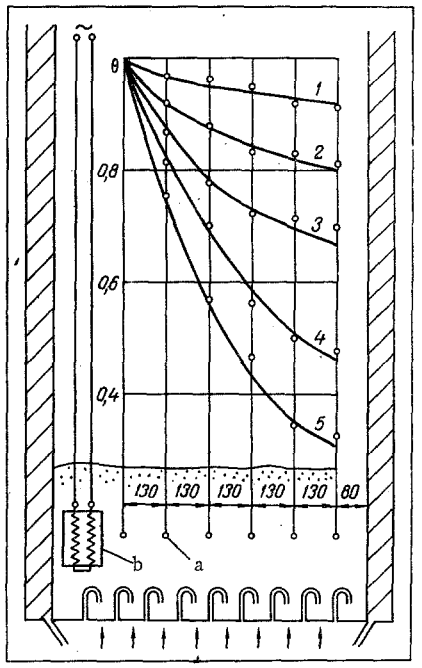

Fig. 1

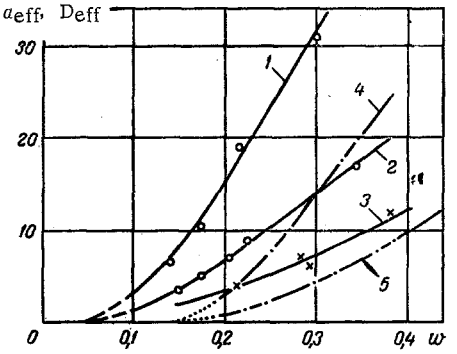

Fig. 2

Fig. 1. Temperature distribution along the test segment in five test runs. 1) H_0 = 0.36 m; w = 0.303 m/sec; $(\theta - t)_{mean}$ = 44°C; a_{eff} = 31.8 cm²/sec; 2) respectively, 0.18; 0.295; 89; 23.8; 3) 0.14; 0.287; 101; 14.1; 4) 0.11; 0.200; 137; 6.06; 5) 0.07; 0.285; 100; 7.33; a) thermocouples; b) heater.

Fig. 2. Heat-transfer coefficients (cm²/sec) as a function of interstitial velocity w (m/sec): 1-3) a_{eff} (d_4 = 90 μ); 4-5) D_{eff} (d_4 = 350 μ) sand [7]; 1) H_0 = 0.37 m; 2) 0.15 m; 3) 0.07-0.1 m; 4) 0.12; 5) 0.06 m.

and temperature, also on the height of the bed. When calculated by the formula $w_0 = w_{0i}(\mu_i/\mu)$ [7], the velocity at which fluidization begins would vary between 0.055 and 0.042 m/sec and the fluidization number between 2.78 and 8.0. The height of the solid bed varied from 0.06 to 0.37 m.

As the electric heater was energized and air was supplied from underneath the grate, a definite temperature profile became established in the chamber. At the beginning of the test the temperature was checked with the control thermocouples once every hour, later with the measuring thermocouples every half hour. A steady state was assumed to have been reached when the temperature at all six points remained the same throughout the last three or four measurements. This corresponded to a balance between the quantity of heat supplied to the bed and the quantity of heat imparted to the air as it is warmed and transmitted through the chamber walls. Owing to the considerable length of the slitted chamber and to the ample power of the heat source, the temperature gradients along the chamber were high (tens of degrees). As a result, possible errors in the determination of temperature values averaged in time at an individual point should have had no significant effect on the accuracy of determining λ_{eff}.

Several curves representing the temperature distribution along the chamber are shown in Fig. 1.

The calculation of a_{eff} is based on the Fourier–Kirchhoff differential equation analogous to the equation which describes the steady-state cooling of a beam. It is assumed that the gas arrives under the grate at a constant temperature t equal to the ambient air temperature, that the gas is uniformly distributed across the chamber section, and that the temperature of the bed varies only between one section perpendicular to the direction of heat flow and another [8], while remaining constant across every section:

$$\frac{d^2(\theta - t)}{dx^2} = \frac{wc_G(\theta - t)}{H\lambda_{eff}} + \frac{2k(\theta - t)}{b\lambda_{eff}}, \quad (1)$$

where

$$k = \frac{1}{1/\alpha_1 + \delta/\lambda + 1/\alpha_2}. \quad (2)$$

TABLE 1

Size of particles	140—160	120—140	100—120	80—100	60—80	40—60	20—40	10—20	10
Weight fraction, %	0,13	2,2	13,2	37,0	37,2	9,1	0,7	0,4	—

Since α_1 is of the order of hundreds of $W/m^2 \cdot deg$ [9], while α_2 is much smaller ($\alpha_2 \approx 10\ W/m^2 \cdot deg$ is assumed in the calculations), the first term in the denominator of (2) may be disregarded.

Solving Eq. (1) with the boundary conditions

$$x = 0; \quad \theta = \theta_1;$$

$$x = l; \quad \left(\frac{d\theta}{dx}\right)_{x=l} = 0$$

(i.e., assuming that the heat losses through the endwall are negligible), we arrive at the following relation:

$$\frac{\theta - t}{\theta_1 - t} = \frac{\mathrm{ch}\,[ml\,[1 - X]]}{\mathrm{ch}\,(ml)}, \tag{3}$$

where

$$m = \sqrt{\left(\frac{wc_G}{H} + \frac{2k}{b}\right)\frac{1}{\lambda_{eff}}}. \tag{4}$$

At $x = l$ ($X = 1$) equality (3) simplifies, to yield a solution for m:

$$m = \mathrm{arch}\,\frac{\theta_1 - t}{\theta_l - t} \cdot l^{-1}. \tag{5}$$

In order to reduce the effect of random errors, m was calculated not only for the first and the last point but also for intermediate points. Since the value of m for the intermediate points could not be expressed in explicit form, the calculations were performed on a Minsk-22 computer, using expression (3) to approximate the temperature distribution curves corresponding to the computed values of m. The computer program provided for a choice of m values such as to distribute the test points relative to the calculated curve (3) according to the rule of least squares.*

In the formula relating the heat-transfer coefficient to the principal fluidized bed parameters it was more expedient to use the thermal diffusivity a_{eff} rather than the thermal conductivity λ_{eff}, because a_{eff} is similar to the diffusivity of the solid phase D_{eff}, thus allowing our experimental results to be compared with those obtained by other authors. Furthermore, the values of a_{eff} – unlike those of λ_{eff} – depend very little on the expansion of the bed and this expansion during fluidization would have been difficult to determine with sufficient accuracy.

From (4), inserting $a_{eff} = \lambda_{eff}/c_M\rho_M(1 - \varepsilon)$ [9] and performing the necessary transformations, we obtain

$$a_{eff} = \frac{wc_G + 2kHb^{-1}}{m^2 c_M \rho_M H_0 (1 - \varepsilon_0)}. \tag{6}$$

An analysis of experimental data has shown that the second term in the numerator of (6) does not exceed 10% of the total and, therefore, a small error in the determination of H should not significantly affect the accuracy of determining a_{eff}.

In Fig. 2 we show the effective thermal diffusivity as a function of w for three different bed heights: 0.08, 0.15, and 0.37 m. At the same time, curves have been plotted here for the thermal diffusivity of the solid phase D_{eff} as a function of the interstitial velocity through sandof the 0.2-0.5 mm size, based on the study by Pippel et al. [10] in which they used a model 400 mm in diameter and made radioactive sodium tracer measurements in the horizontal direction for some definite length of time after it had been injected into the bed. As can be seen here, the order of magnitude of a_{eff} and D_{eff} as well as the character of their dependence on w are similar.

* The program was designed, the m values were computed, and the critical relation based on test points was found by co-workers of the YuzhNIIGIPROGaz A. S. Aptekar, V. G. Yasenko, Z. N. Pancheva, and V. I. Pischasova.

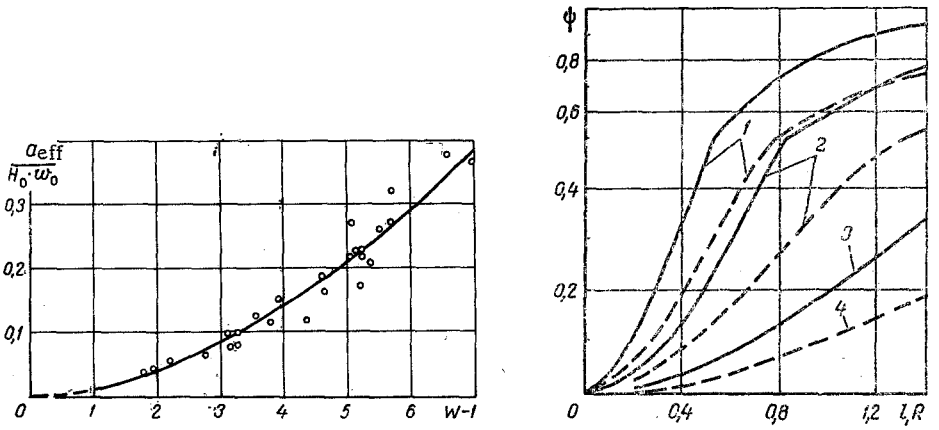

Fig. 3. Correlation between the generalized formula $a_{eff}/H_0w_0 = 0.0115\ (W - 1)^{1.8}$ and experimental results.

Fig. 4. Calculated nonuniformity factor of the temperature field as a function of the chamber dimensions according to design. Values of λ_{eff} and m taken from tests (solid line for a parallelepiped, dashed line for a cylinder): for test No. 16 [1] H = 0.115 m; w = 0.164 m/sec; λ_{eff} = 290 W/m · deg; m = 2.53 m^{-1}; for test No. 20: 2) respectively, 0.175; 0.180; 560; 1.55; for test No. 12: 3) 0.420; 0.123; 775; 0.700; for test No. 13: 4) 0.300; 0.276; 2400; 0.705].

In the general case a_{eff} is a function of several independent variables:

$$a_{eff} = f(w,\ H_0,\ \rho_M,\ \rho_G,\ \nu,\ d_p,\ g). \tag{7}$$

According to the π-theorem, there should be 8 − 3 = 5 dimensionless ratios here. Based on a dimensional analysis and considering the effect of various parameters [11] on the value of a_{eff}, we arrive at the following relation:

$$\frac{a_{eff}}{H_0 w_0} = N(W-1)^{n_1}\,\mathrm{Ar}^{n_2}\left(\frac{H_0}{d_p}\right)^{n_3}\mathrm{Fr}_0^{n_4}. \tag{8}$$

The Froude number $\mathrm{Fr}_0 = w_0^2/d_p g$ remained almost constant and equal to 2.66 throughout the tests. The other quantities in Eq. (8) varied as follows: $(W - 1) = (w/w_0 - 1)$ from 1.78 to 7.0; H_0/d_p from 670 to 4100; $\mathrm{Ar} = (gd_p^3/\nu^2)(\rho_M/\rho_G)$ from 29 to 78; a_{eff}/H_0w_0 varied from 0.038 to 0.42.

The power exponents and the coefficient m were calculated on a Minsk-22 computer according to the multiple-correlations program. As a result, the following equation was obtained:

$$\frac{a_{eff}}{H_0 w_0} = 8\cdot 10^{-3}(W-1)^{1.8}\,\mathrm{Ar}^{-0.009}\left(\frac{H_0}{d_p}\right)^{0.049}, \tag{9}$$

valid for $\mathrm{Fr}_0 = 2.66$. With an error not greater than 5% (within the given ranges of the variables), it could be replaced by a simpler formula:

$$\frac{a_{eff}}{H_0 w_0} = 0.0115(W-1)^{1,8}. \tag{10}$$

In Fig. 3 formula (10) has been correlated with the experiment. The maximum deviation of test points from curve (10) was 28%.

The values of a_{eff} calculated according to (10) ranged from 5 to 35 cm^2/sec and the corresponding values of λ_{eff} from 290 to 2400 W/m · deg.

With the λ_{eff} range known, it is possible to evaluate the nonuniformity of the temperature fields. From Eq. (3), at X = 1 and without losses through the walls, we have obtained:

$$\psi = \frac{\theta_1 - \theta_l}{\theta_1 - t} = 1 - \left[\mathrm{ch}\left(l\sqrt{\frac{wc_G}{H\lambda_{eff}}}\right)\right]^{-1}. \tag{11}$$

In industrial furnaces the heat may be supplied through the wall of the cylindrical chamber. For this case the solution to the Fourier equation at r = 0 is

$$J_0(m_1R) = \frac{\theta_1 - t}{\theta_0 - t}, \tag{12}$$

where $J_0(m_1R)$ is the second-order modified Bessel function of the first kind with

$$m_1 = \sqrt{\frac{wc_G}{H\lambda_{eff}}}. \tag{13}$$

The Bessel function will now be replaced by the corresponding series [12]:

$$\theta_0 = t + \frac{\theta_1 - t}{1 + \frac{(m_1R)^2}{2^2} + \frac{(m_1R)^4}{2^2 4^2} + \dots}. \tag{14}$$

Retaining only the first two terms of this series, which is permissible (with an error not exceeding 5%) for $m_1R \leq 1.4$, we have substituting for m_1 from (13):

$$\lambda_{eff} = \frac{wc_GR^2}{4H} \cdot \frac{\theta_0 - t}{\theta_1 - \theta_0}. \tag{15}$$

An appropriate transformation yields for a cylindrical fluidization chamber:

$$\psi = \frac{wc_GR^2}{4H\lambda_{eff} + wc_GR^2} = \left(\frac{4}{m^2R^2} + 1\right)^{-1}. \tag{16}$$

The condition $m_1R \leq 1.4$ or its equivalent $\lambda_{eff} \geq wc_GR^2/1.96H$ is usually satisfied in large chambers with heavy circulation systems [2]. According to the data in [1, 5, 8], λ_{eff} is of the order of hundreds or even thousands of W/m·deg. It is not difficult to verify that $\lambda_{eff} = wc_GR^2/1.96H$ for any even quite arbitrarily chosen values of w and H within the ranges under consideration here.

In Fig. 4 we show how ψ depends on the radius (half-length) of the chamber at various values of H, w, and λ_{eff} taken from our test data.

For illustration, we will now determine the nonuniformity factor in an alumina dehydration chamber where the bed is heated by means of tunnel burners mounted in the sidewalls $2l = 5$ m apart according to design. If $H_0 = 0.8$ m, $w = 0.3$ m/sec, $\theta_{mean} = 500°C$, $H/H_0 = 1.3$, and $\lambda_{eff} = 2400$ W/m·deg (maximum values obtained in our tests), then

$$m = \sqrt{\frac{0.3 \cdot 1300 \cdot 273}{(500 + 273) \cdot 0.8 \cdot 1.3 \cdot 2400}} = 0.24\ \text{m}^{-1}.$$

At the same time, $\psi = 0.15$. This means that deviations from the mean temperature amount to $\Delta\theta/2 = \theta_{mean} \cdot \psi/2 = 40°C$. Consequently, the lowest temperature (at the center) is approximately 460°C and the highest temperature (near the wall) is approximately 540°C.

NOTATION

b	is the width of the chamber;
l	is the length of the chamber heated from one end, or the half-length of the chamber heated from both ends;
H_0, H	are the heights of the solid and the fluidized bed, respectively;
w	is the interstitial velocity;
w_{0i}, w_0	are the interstitial velocities at which fluidization begins at initial and at operating temperature, respectively;
W	is the fluidization number;
x, r	are the space coordinates;
$X = x/l$	is a dimensionless coordinate;
$Z = H/H_0$;	
c_G, c_M	are the specific heat of the gas and of the bed material, respectively;
k	is the heat-transfer coefficient;
α_1, α_2	are the heat-transfer coefficients at the inner and outer surface of a chamber, respectively;
δ	is the chamber wall thickness;
λ	is the thermal conductivity of the wall material;

t	is the air temperature under the grate;
θ, θ_1, θ_l, θ_0	are the temperatures of the fluidized bed: mean, at the initial point, at the end of the slitted chamber, and at the center of the cylindrical chamber, respectively;
$\theta = (\theta - t)/(\theta_1 - t)$	is the dimensionless excess temperature;
ε_0, ε	are the porosity of the solid and the fluidized bed, respectively;
λ_{eff}	is the effective thermal conductivity;
a_{eff}	is the effective thermal diffusivity;
ρ_G, ρ_M	are the densities of the gas and of the bed material, respectively;
ν	is the kinematic viscosity;
μ_i, μ	are the dynamic viscosities under initial and operating conditions, respectively;
d_p	is the diameter of the particles;
$\psi = \Delta\theta/(\theta_1 - t)$	is the nonuniformity factor of the temperature field.

LITERATURE CITED

1. I. G. Martyushin et al., Khim. Promyshl., No. 6 (1968).
2. M. É. Aérov and O. M. Todes, Hydraulic and Thermal Aspects in the Operation of Apparatus with a Steady and Boiling Granular Bed [in Russian], Khimiya (1968).
3. V. A. Borodulya and A. I. Tamarin, Inzh.-Fiz. Zh., No. 11 (1962).
4. V. A. Borodulya, Inzh.-Fiz. Zh., No. 8 (1963).
5. V. A. Borodulya, S. S. Zabrodskii, A. I. Tamarin, and V. I. Yuditskii, in: Heat and Mass Transfer [in Russian], Vol. 5, Énergiya, Minsk (1966).
6. W. Lehman, F. Mueller, W. Schramm, et al., Chem. Tech., No. 11 (1969).
7. S. S. Zabrodskii, Hydrodynamics and Heat Transfer in a Fluidized Bed [in Russian], Gosénergoizdat (1963).
8. K. Peters, A. Orlichek, and A. Schmidt, Chem. Ing. Tech., 25, No. 6, 313 (1953).
9. N. I. Gel'perin, V. G. Ainshtein, and V. B. Kvasha, Fundamentals of Fluidization Technology [in Russian], Khimiya, Moscow (1967).
10. W. Pippel et al., Chem. Tech., No. 12 (1968).
11. K. O. Bennet and G. E. Mayers, Hydrodynamics, Heat and Mass Transfer [Russian translation], Nedra, Moscow (1966).
12. H. Carslow and T. Eger, Operational Methods in Applied Mathematics [Russian translation], IL, Moscow (1948).